New Accurate 3-D Finite Element Technology for Solving Geometrically Complex Coupled-Field Problems

I. Avdeev[*], M. Gyimesi[**], M. Lovell[*] and D. Ostergaard[**]

[*]University of Pittsburgh, Pittsburgh, PA, USA, mlovell@pitt.edu
[**]ANSYS, Inc., Canonsburg, PA, USA, miklos.gyimesi@ansys.com

ABSTRACT

A novel 3-D transducer formulation has been developed to solve geometrically complex coupled-field problems. The transducer is compatible with both structural and electrostatic solid elements, which allows for modeling complex devices. Through internal morphing capabilities and exact element integration the 3-D transducer element is one of the most powerful coupled field FE analysis tools available. To verify the accuracy and effectiveness of 3-D transducer a series of benchmark analyses were conducted.

Keywords: MEMS, FEA, coupled-field, 3-D transducer

1 INTRODUCTION

The increased functionality of MEMS fabrication and production techniques has lead to the ability of creating devices and components with complex geometrical configurations. These components require efficient FE modeling techniques to solve coupled electromechanical problems. The lumped models are no longer applicable for devices, such as combdrives or electrostatic motors, where fringing electrostatic fields are dominant [1]. There have been several numerical methods proposed for the treatment of electromechanical systems including: FE or boundary element methods using sequential physics coupling; strongly coupled but reduced order methods using fully lumped or mechanically distributed but electrically lumped 1-D, multi-dimensional or modal-space transducers. All of these methods need some extra meshing or morphing, introduce simplifying assumptions and may not be convenient to use [2].

In the present investigation, a novel strongly coupled 3-D tetrahedral transducer element is introduced for modeling analog electrostatic MEMS devices. This new transducer element, which can be utilized for a broad range of micro-system applications (combdrives, micromirrors, and electrostatic motors), is compatible with conventional electrostatic and structural 3-D finite elements. The element is capable of efficiently modeling interaction between deformable or rigid conductors that generate an electrostatic field. Strong coupling between the electrostatic and mechanical domains allows the static element formulation to be extended to transient and full harmonic analyses. Therefore, in many respects, the element is the most sophisticated FEA tool available for modeling MEMS problems where dominant fringing fields develop. The new technology is also very efficient in determining the pull-in parameters of complicated multi-electrode microdevices.

2 COUPLED-FIELD FE FORMULATION

The electrostatic 3-D domain of a coupled-field electro-mechanical problem is meshed with the new 3-D elements. The 3-D transducer element has a tetrahedral shape with the geometry fully defined by four nodes (see Figure 1).

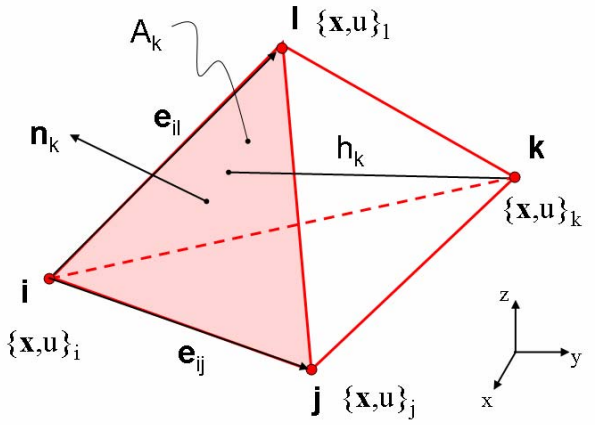

Figure 1: 3-D transducer element geometry and degrees of freedom (mechanical displacements and electrostatic potentials).

Each element node has four degrees of freedom: three components of a nodal displacement vector defined in a global Cartesian coordinate system, $\mathbf{x} = (u_x,u_y,u_z)$, and one potential of electrostatic field, u. There are three mechanical forces associated with each node: F_x, F_y, and F_z, and a nodal charge, Q. Transducer element potential energy is given by

$$W_e = \frac{\varepsilon}{2}\int_V \mathbf{E}^2 dv = \frac{\varepsilon}{2}\int_V (gradU)^2 dv \qquad (1)$$

In (1), ε is the element permittivity (assumed constant for the sake of simplicity), V is the element volume, $\mathbf{E}$ is the electrostatic field intensity vector, and U is the electrostatic

potential. For a linear tetrahedral element the integral in (1) can be evaluated analytically:

$$W_e = \frac{V\varepsilon}{2}(gradU)^2 = \frac{V\varepsilon}{2}\sum_{i=1}^{4}\sum_{j=1}^{4}\frac{\mathbf{n}_i \cdot \mathbf{n}_j}{h_i h_j}u_i u_j \qquad (2)$$

In (2), h_i are the tetrahedral altitudes, $\mathbf{n}_i$ are the element's face normals, and u_i are the nodal electrostatic potentials. The energy is a function of the element geometry and nodal potentials. One of the important results is that (2) is an invariant formula for energy calculation. The mechanical forces and electrical charges in the element are calculated using virtual work principle [3]. The vectors of nodal mechanical forces and charges are calculated using the principle of virtual work by differentiating the element energy with respect to nodal mechanical displacements and electrostatic potentials [3]. The static non-linear equilibrium equations for the electrostatic domain meshed with transducer elements can be written in an incremental form suitable for the Newton-Raphson equation solvers

$$\begin{bmatrix}\mathbf{K}_{xx}(\mathbf{x},\mathbf{u}) & \mathbf{K}_{xu}(\mathbf{x},\mathbf{u})\\ \mathbf{K}_{ux}(\mathbf{x},\mathbf{u}) & \mathbf{K}_{uu}(\mathbf{x},\mathbf{u})\end{bmatrix}\begin{bmatrix}\Delta\mathbf{x}\\ \Delta\mathbf{u}\end{bmatrix} = \begin{bmatrix}\Delta\mathbf{f}(\mathbf{x},\mathbf{u})\\ \Delta\mathbf{q}(\mathbf{x},\mathbf{u})\end{bmatrix} \qquad (3)$$

In (3), $\Delta\mathbf{x}$ and $\Delta\mathbf{u}$ are the increments of vectors of the nodal mechanical displacements and electrostatic potentials, $\Delta\mathbf{f}(\mathbf{x},\mathbf{u})$ and $\Delta\mathbf{q}(\mathbf{x},\mathbf{u})$ are the increments of the out-of-balance nodal forces and charges respectively. The blocks of the coupled-field tangent stiffness matrix in (3) are computed by differentiating nodal forces and charges with respect to nodal mechanical displacements and electrostatic potentials [3]. To increase accuracy and to ensure a robust convergence of the non-linear solution, the integrals and derivatives of the element's formulation are calculated analytically.

3 MESH MORPHING

An internal mesh morphing capability is an important feature of the developed transducer element that separates it from lumped transducers and models based on a sequential coupling. Mesh morphing is a process of updating vectors of nodal displacements of the transducer elements during the solution of a non-linear problem. The number of elements remains constant so that element continuity is maintained during mesh morphing. In the element, there are out-of-balance mechanical forces acting upon each node. The interface nodes (nodes on the surface of electrodes) generate the electrostatic force that deforms the mechanical structure. Every inner node moves in a direction defined by the resulting out-of-balance force acting upon the node.

Structural stiffness of the transducer elements is inversely proportional to the element volume, i.e. the bigger elements are softer than the smaller ones. This is extremely important for modeling geometrical singularities such as sharp corners or edges. The mesh must be refined around the singularities in order to capture strong electrostatic fields and to accurately compute driving forces. High forces, however, can "invert" transducer elements if their structural stiffnesses are not big. For this reason, the structural stiffness of transducers is weighted based on their size (volume).

The convergence speed and solution accuracy of the element during a non-linear solution depends on many parameters, the most important of which are the convergence tolerance (CT) and the morphing acceleration factor (MAF). The first parameter is a convergence criterion used by an iterative Newton-Raphson solver. The second parameter is a factor used to stiffen or soften all of the transducer elements. Increasing the morphing acceleration factor produces a stiffer mesh, which could be necessary for strong singularities or small displacements.

4 NUMERICAL EXAMPLES

Several benchmark problems are solved using the new 3-D transducer element. The results are compared to experimental data available in the literature and to the solutions obtained using traditional techniques and commercial software (such as ANSYS\Multiphysics).

4.1 Parallel Plate Capacitive Transducer

As a first example to demonstrate the new element capabilities, we will compute a static equilibrium state of a parallel plate capacitive transducer [2]. The transducer consists of two electrodes separated by a gap that is a function of applied voltage and a stiffness of the suspending spring. This problem has an analytical solution for rigid electrodes and a lumped spring without accounting for fringing electrostatic fields [2]. The FE model consists of 100 transducers and one spring element (Figure 2).

CT	Time (s)	Iterations	Stroke	Error (%)
0.02000	2.84	7	0.16989	15.06
0.00500	3.71	12	0.19184	4.08
0.00050	5.34	21	0.19914	0.43
0.00005	6.97	30	0.19991	0.05

Table 1: Solution convergence speed and accuracy for various convergence tolerance (CT) values.

The electrostatic potential distribution is depicted in Figure 2. In Table 1, the solution accuracy and speed are compared for different values of convergence tolerance (morphing acceleration factor is set to one). At a smaller value of the tolerance, more iterations are required to converge, but the solution becomes more accurate. This is an intuitively simple, but very important result. In Table 2, the solution accuracy and speed are compared for different

values of morphing acceleration factor (convergence tolerance is equal to 0.00005 N).

MAF	Time (s)	Iterations	Stroke	Error (%)
0.25	4.51	16	0.19991	0.05
1.00	6.97	30	0.19991	0.05
4.00	17.16	85	0.19990	0.05

Table 2: Table 4: Solution convergence speed and accuracy for various morphing acceleration factor (MAF) values

A smaller factor (softer mesh) leads to a faster convergence, while a larger factor leads to a slower convergence. Note, that the accuracy essentially remains independent of the acceleration factor.

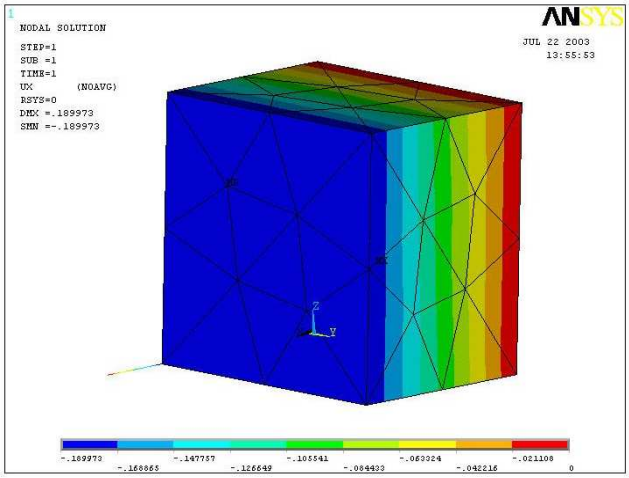

Figure 2: Parallel plate transducer: electrostatic potential distribution (3-D).

To achieve more accurate solution, one must therefore adjust the value of the convergence tolerance. The MAF can be further used to speed up the convergence for a given accuracy. It should be noted that there is a bottom MAF limit which cannot be reached without loosing the integrity of the transducer elements (transducer FE mesh becomes too soft mechanically). This limit varies for different problems and boundary conditions.

4.2 Electrostatic Torsion Microactuator

The second example problem that will be used to verify the 3-D transducer is an electrostatic torsion microactuator [4]. The finite element model of the microactuator is depicted in Figure 3. Structural brick elements (green) were used to model the microactuator. The 3-D transducer elements (purple) were used to model air gap between two driving electrodes and the actuator's plates. FE model contains 5,207 transducers and 2,096 structural ANSYS finite elements.

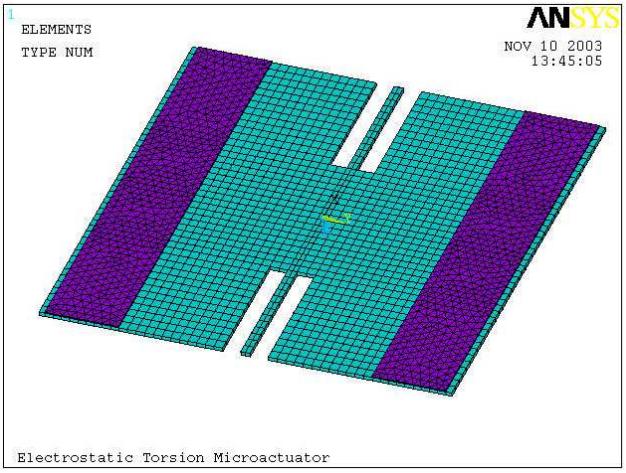

Figure 3: Electrostatic torsion microactuator: structural brick and transducer tetrahedral finite elements.

Alternating voltage between the two electrodes allows the micromirror to turn around the supporting beam axis. Increasing voltage leads to pull-in of the micromirror.

	Theory [4]	Experiment [4]	FEA (3-D)
θ_{pin}, (deg)	0.4042	0.385	0.397
V_{pin} (V)	11.59	11.50	11.55

Table 3: Comparison of theoretical, experimental, and FE pull-in parameters for torsion microactuator

The reported theoretical and experimental values of pull-in voltage are presented in Table 3. The results obtained using the 3-D transducer model are compared to the reported results. The FE results show very good agreement with the theoretical and experimental data [4].

4.3 Lateral Combdrive Transducer

The lateral combdrive electromechanical transducer [5] (Figure 4) is the final example problem to be solved with the new transducer element. FE coupled model contains 12,740 transducer elements. Structural domain is assumed to be rigid. Boundary conditions play an important role in the modeling and solution. The external nodes of the transducer mesh are free to move, while the boundary is fixed in certain directions. The outside boundary (far-field) is fixed with respect to all mechanical displacements. A voltage is applied between the rotor and the stator that produces strong fringing fields with potential distribution depicted in Figures 5 and 6. The mechanical displacement field along the combdrive axis is depicted in Figure 7 (surrounding air is hidden in the figure). The combdrive stroke as a function of the applied voltage was compared to semi-analytical solution and was found to be in a good agreement with it for a carefully chosen convergence tolerance parameter [2].

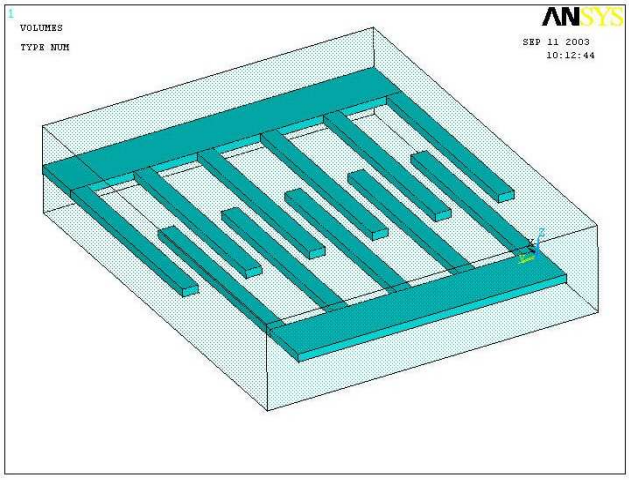

Figure 4: 3-D CAD model of the combdrive transducer.

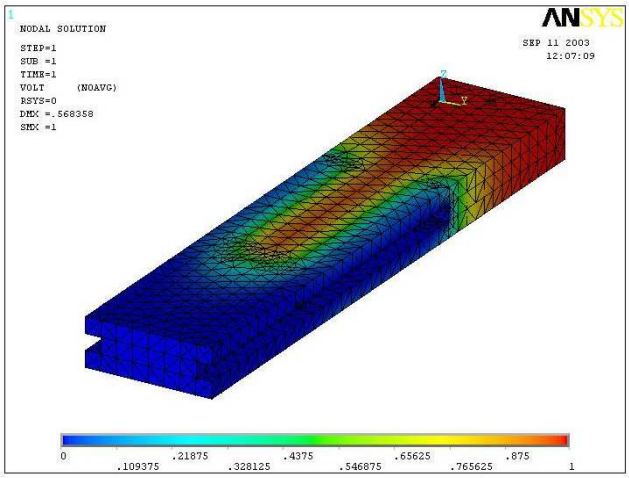

Figure 5: 3-D electrostatic potential distribution of a representative combdrive finger including surrounding air.

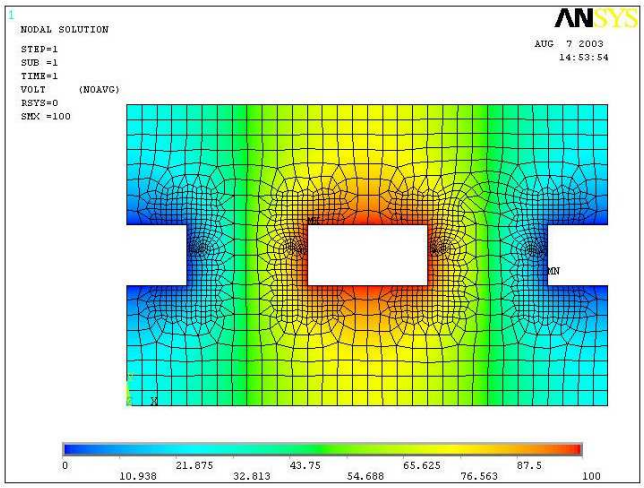

Figure 6: Potential distribution in the middle of the combdrive finger (2-D cross-section).

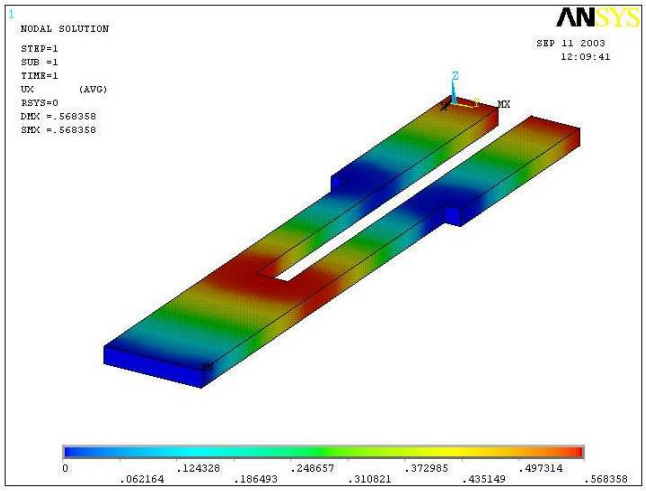

Figure 7: Mechanical displacement field along the combdrive finger axis (stroke).

5 CONCLUSIONS

A distributed 3-D transducer element formulation was developed for modeling a wide range of MEMS devices. The elements accounts for fringing electrostatic fields and the internal morphing capability of the element allows a designer to use the original mesh for solving large displacement non-linear problems. The computer FE code was developed using ANSYS as a platform and several numerical examples were presented which show good agreement with experimental data. The developed element is among the most sophisticated and effective techniques of solving 3-D coupled field problems presently available for designers and researchers working in the MEMS industry.

REFERENCES

[1] I. Avdeev, M. Lovell and D. Onipede, Jr., "Modeling In-Plane Misalignments in Lateral Combdrive Transducers," J. of Micromechanics and Microengineering, V.13, pp. 809-15 (2003).

[2] I. Avdeev, "New Formulation for Finite Element Modeling Electrostatically Driven MEMS," Ph.D. dissertation, University of Pittsburgh (2003).

[3] M. Gyimesi, D. Ostergaard and I. Avdeev, "Triangle Transducer for MEMS Simulation in ANSYS Finite Element Program," Proc. of the Fifth Int. Conf. on Model. Simulat. of Microsystems, San Juan, PR, April 22-25, pp. 380-83 (2002).

[4] O. Degani, E. Socher, A. Lipson, T. Leitner, D. Setter, S. Kaldor and Y. Nemirovsky, "Pull-in Study of an Electrostatic Torsion Microactuator," J. Microelectromech. Syst. V. 7, pp. 373–77, (1998).

[5] W. Tang, T. Nguyen and R. Howe, "Laterally driven polysilicon resonant microstructures," Sensors and Actuators A, V. 20, pp. 25–32 (1989).